

## Scallop Shells Exhibit Optimization of Riblet Dimensions for Drag Reduction

ERIK J. ANDERSON, PATRICK S. MACGILLIVRAY, AND M. EDWIN DEMONT\*

*Biology Department, St. Francis Xavier University, Antigonish, Nova Scotia, Canada B2G 2W5*

*Drag reduction by streamwise surface grooves, or riblets, has been observed by engineers and has been suggested to apply to certain biological systems. Drag reductions as high as 8% have been observed (1), leading to practical nautical and aeronautical applications (2, 3, 4). The shells of several species of scallop, including *Placopecten magellanicus*, display riblets arranged radially, and therefore roughly parallel to the flow during swimming (Fig. 1a). The dimensions of these riblets on particular scallops fall within the region necessary for drag reduction at experimentally measured swimming speeds. Moreover, the actual spacing of the riblets gradually migrates into the theoretically optimal spacing region as shell length increases beyond 40 mm (Figs. 2, 3). Specimens of *P. magellanicus* 40 to 80 mm in length demonstrate the greatest swimming ability (5); our data strongly suggest that streamwise riblets may be a contributing factor to the swimming success in scallops of this size range.*

The giant scallop, *Placopecten magellanicus*, was the subject of a recent comprehensive work on the hydrodynamics and energetics of locomotion (6, 7, 8, 9). Scallops utilize a jet-propulsion system in swimming: water is taken in when the shells open, and the valve-like velum traps a volume of water between the shells which is expelled in two jets adjacent to the hinge as the shells clap shut. The scallop is therefore propelled through the water gape-leading, hinge-trailing, at speeds up to about 0.55 m/s, the swimming speed common to scallops 65 mm in ventral-dorsal length,  $L_s$  (5). Their swimming ability enables scallops to escape from predators, such as starfish, and, as some suggest, to migrate with the seasons (5). Certainly if the

latter behavior were a significant part of the scallop life cycle, development of drag-reducing structural features would not be surprising.

Recent years have seen the application of streamwise grooves, or riblets, to aircraft and the hulls of racing boats as a means of drag reduction and, therefore, enhanced speed capability and decreased energy requirements. The mechanism involves a reduction in the surface shear stress arising from a turbulent boundary layer. Similar grooves in aquatic organisms may offer the same advantage (3, 4, 10, 11). We examined about 440 species of bivalves from 60 families representing over 160 genera and found that, with the exception of 7 genera, radial riblets of dimensions similar to those in *P. magellanicus* occur almost exclusively in swimming bivalves (observed in 16 genera). The *Limidae*, which swim hinge first, in the direction opposite to that of the scallop, also exhibit radial riblets.

Theoretical and experimental work by fluid engineers has elucidated the function and efficacy of riblets (12, 13) with drag reductions of 3%–8% observed in various systems, from flat plates, to the hulls of racing boats (2), the surfaces of aircraft (3), and the skin of sharks (3, 4, 10, 11). Though riblet function is still not fully understood, researchers have put forth a theory, based on the organization of surface vortices, to explain the drag-reducing mechanism. According to the theory, there is a reduction in the component of drag arising from a particular high shear occurrence generated by the action of so-called hairpin vortex tubes. In turbulent boundary layers, hairpin-shaped vortex tubes occur near the surface, oriented so the bend of the hairpin is downstream and the two prongs of the hairpin are pointed upstream and aligned roughly parallel to the flow. As the bend of the hairpin is swept further downstream, the remaining vortex tubes move toward each other in a spanwise direction, which

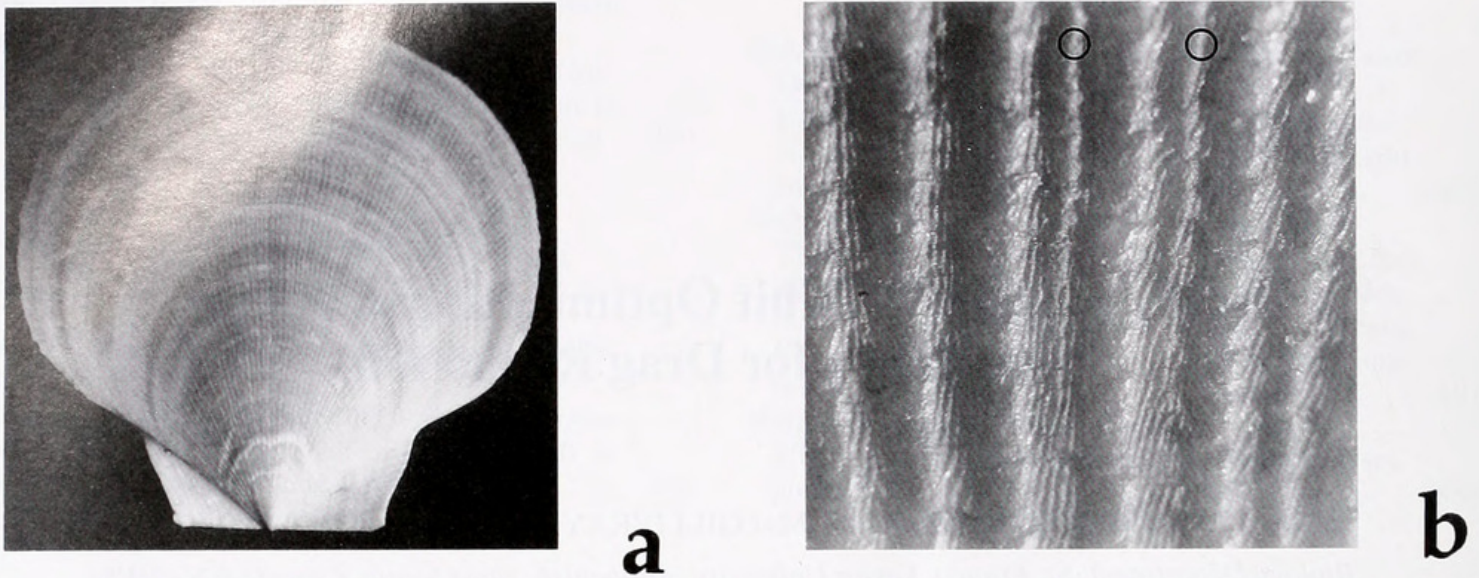


**Figure 1.** Photographs of riblets on the scallop *Placopecten magellanicus*. (a) Whole shell. Shell length,  $L_s = 63$  mm. (b) Magnified image of riblets. Note the two newly added riblets marked with circles. For scale, the distance between the two circles is 1 mm.

ultimately results in a downwash of fluid onto the surface. This phenomenon is known as near-wall burst. Riblets may inhibit this spanwise movement by organizing

adjacent surface vortex tubes into streamwise corridors and thus restricting the vortex tubes from interacting to cause near-wall burst.

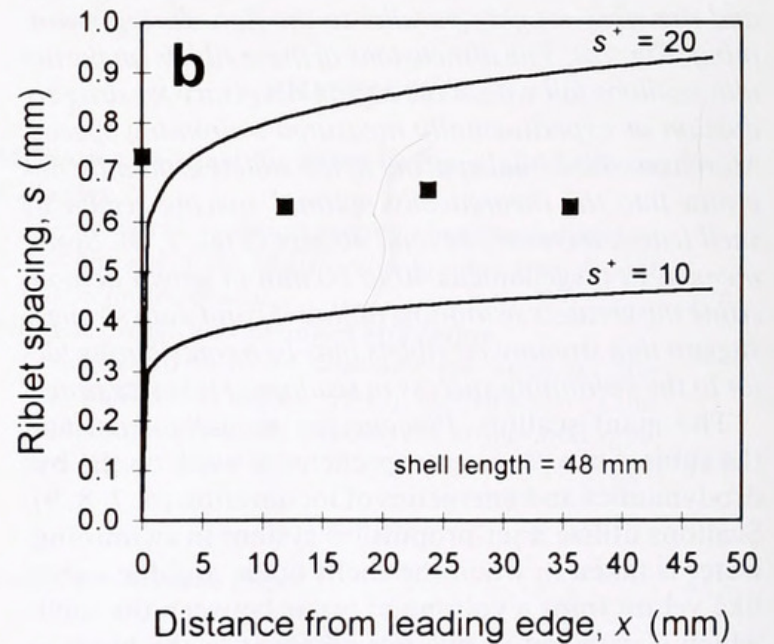
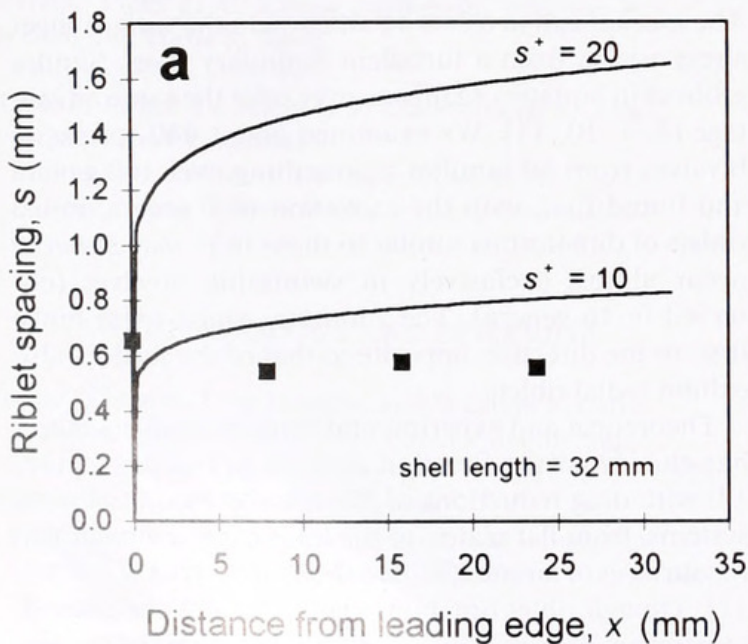


**Figure 2.** Real riblet spacings (squares), at positions  $x = 0, 0.25L_s, 0.5L_s,$  and  $0.75L_s$ , plotted against distance from the leading edge of the shell, from two representative scallops: (a)  $L_s = 32$  mm; (b)  $L_s = 48$  mm. The solid lines represent the boundaries of the optimal riblet spacing region for riblet-based drag reduction, which is specific to each scallop on the basis of shell length and swimming speed (Eqs. 1 and 2). A series ( $n = 20$ ) of *P. magellanicus* shells of  $L_s$ , from 10 mm to 90 mm was used in this study. Arcs were established at positions  $x = 0, 0.25L_s, 0.5L_s,$  and  $0.75L_s$ , over the central 30 degree sector of each shell, and the number of riblets on each arc was counted; Bioquant OS/2 image analysis software was used for positioning and counting. Real riblet spacings were calculated by dividing the arc length,  $l_{arc} = \pi(L_s - x)/6$ , at each of the four positions by the number of riblets on the arc. Swimming velocities, needed to calculate wall shear stresses (Eq. 2), vary significantly with shell length and were taken from published data obtained from film of *P. magellanicus* swimming *in situ* (5). Note that despite the radial pattern of riblets, spacing remains relatively constant due to riblet addition. Note also that the spacing measurements move into the optimal region between  $s^* = 10$  and  $s^* = 20$  as shell length increases from 32 mm to 48 mm.

Riblet spacing for optimal drag reduction can be determined from the following expression,

$$s = \nu s^+ \sqrt{\frac{\rho}{\tau_w}} \quad (\text{Eq. 1})$$

where  $s$  is actual riblet spacing,  $\nu$  is the kinematic viscosity of the fluid,  $s^+$  is a dimensionless expression of riblet spacing for which the range 10–20 has been determined to be optimal (11, 14),  $\tau_w$  is the wall shear stress due to the flow, and  $\rho$  is the fluid density. The equation is simply a rearrangement of the standard expression for a dimensionless length parameter, in terms of  $\nu$ ,  $\tau_w$  and  $\rho$ . Such dimensionless parameters are used in fluid dynamics for the reason that, in general, any two systems with the same  $s^+$  value will behave similarly, though values of actual spacing,  $s$ , may differ. Wall shear stress for the swimming scallop was determined from the equation for flow over a flat plate with a turbulent boundary; the equation was obtained through the standard practice of applying the momentum integral equation to a  $1/7$  power velocity profile,

$$\tau_w = \frac{1}{2} \rho U^2 \frac{0.0594}{Re_x^{1/5}} Re_x = \frac{Ux}{\nu} \quad (\text{Eq. 2})$$

where  $U$  is the flow velocity over the scallop,  $Re_x$  is the length (or local) Reynolds number, and  $x$  is the distance measured along the line bisecting the valve, starting from the most ventral edge of the valve (*i.e.*, the leading edge of the scallop). Due to the shell curvature, the shear would be slightly higher than the equation predicts for the leading section of the scallop. A turbulent boundary layer is assumed on the basis of Reynolds numbers close to the transition between laminar and turbulent flow; an early breakdown of the laminar boundary layer is probably triggered by the combined effects of leading edge roughness and the rapid clapping of the leading edge of the scallop during swimming.

The average riblet spacing as a function of distance from the leading edge was determined for each scallop observed, then plotted together with the theoretically predicted optimal riblet spacing for  $s^+ = 10$  and  $s^+ = 20$  (Fig. 2). At smaller shell lengths, the actual riblet spacing data fall below the optimal region (Fig. 2a). Since scallops of lengths up to about 30 mm are attached to the ocean bottom by byssal threads (5), there would be no advantage for optimized riblet spacing in these smaller scallops. At a shell length of about 50 mm—the size at which *P. magellanicus* exhibits the greatest swimming speed (in body lengths per second)—the actual riblet spacing data fall near the center of the optimal region for riblet-based drag reduction (Fig. 2b). When the riblet spacing at  $x = 0.5L_s$  for each scallop observed is plotted against shell length, the riblet spacing on scallop shells larger than 40 mm remains in the optimal region (Fig.

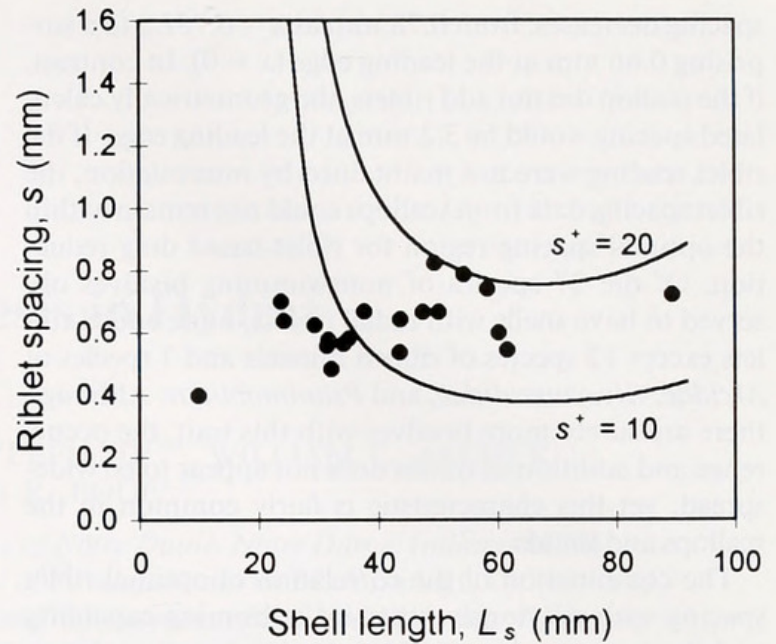


**Figure 3.** Real riblet spacing at position  $x = 0.5L_s$ , plotted against shell length. The plot compares the riblet spacings of the entire series ( $n = 20$ ) of shells observed at the same relative position on each shell. Thus, each data point (circle) is produced from the spacing data of a different shell. The solid lines are the predicted optimal riblet spacing for  $s^+ = 10$  and  $s^+ = 20$ , at  $x = 0.5L_s$ , using swimming speeds corresponding to the given shell lengths (5). Notice that as shell length increases past 40 mm, the data points enter the optimal region.

3). Moreover, the higher Reynolds numbers,  $Re = 2.0\text{--}4.0 \times 10^4$ , at these larger scallop sizes, increase the likelihood of transition from laminar to turbulent boundary flow. Thus, scallops of the size reported to swim most vigorously are highly favored for riblet-based drag reduction, suggesting an optimization of shell design. Research on *P. magellanicus* reveals that scallops larger than 80 mm are generally less active swimmers due to inferior hydrodynamic characteristics and heavy bodies (5, 7). Scallops of this size are also commonly covered with embionts which reduce swimming ability.

An equally impressive aspect of riblet design in these scallops is best introduced by examining the equations for determining optimal riblet spacing,  $s$ . Combining equations 1 and 2 reveals that optimal riblet spacing is inversely proportional to distance from the leading edge to the  $1/10$  power. Therefore, as the optimal curves show (Fig. 2), the best arrangement would be to have, at the leading edge of an object ( $x = 0$ ), narrow spacing which gets wider as you move toward the trailing edge ( $x = L_s$ ). The radial pattern of the scallop riblets, which has its vertex at the trailing edge, would be the opposite of this optimal arrangement if it were not for the fact that riblets are added to the pattern, by intercalation, as the scallop grows (Fig. 1b); *i.e.*, there are more riblets at the leading edge than near the vertex. Shells showed an average of 3 to 4 times as many riblets at the leading edge as at  $x = 0.75L_s$ . For example, in a shell 54 mm in length, riblet

spacing decreases, from 0.78 mm at  $x = 0.75L_s$ , to a surprising 0.66 mm at the leading edge ( $x = 0$ ). In contrast, if the scallop did not add riblets, the geometrically calculated spacing would be 3.2 mm at the leading edge. If the riblet spacing were not maintained by intercalation, the riblet spacing data from scallops could not remain within the optimal spacing region for riblet-based drag reduction. Of the 37 species of nonswimming bivalves observed to have shells with radial riblets, none added riblets except 12 species of ribbed mussels and 7 species of *Arcidae*, *Glycymerididae*, and *Psammobiidae*. Although there are surely more bivalves with this trait, the occurrence and addition of riblets does not appear to be widespread; yet this characteristic is fairly common in the scallops and limids.

The combination of the correlation of optimal riblet spacing with previously observed swimming capability and the maintenance of riblet spacing by intercalation implies that the apparent fine-tuning of riblet spacing on *P. magellanicus* is functionally significant.

#### Acknowledgments

This research was funded by an NSERC (Canada) research grant to M.E.D. P.S.M. was supported by an NSERC Summer Research Scholarship. We thank R. Antonia (The University of Newcastle) for his valuable comments and suggestions throughout this study, A. Anderson (St. F. X.) for the use of his image analysis equipment, the Nova Scotia Museum of Natural History for opening their bivalve collection to us, E. Kechington at the Department of Fisheries and Oceans for sending specimens, and collector M. Le Quement for his contri-

bution of bivalves from Brittany. We thank also J. Flynn (Dalhousie), W. Quinn (St. F.X.) and S. Vogel (Duke) for reading the manuscript.

#### Literature Cited

1. Walsh, M. J., and L. M. Weinstein. 1978. Drag and heat transfer on surfaces with longitudinal fins. *AIAA Paper* 78-1161.
2. Bushnell, D. M., and K. J. Moore. 1991. Drag reduction in nature. *Annu. Rev. Fluid Mech.* 23: 65-79.
3. Moin, P., and J. Kim. 1997. Tackling turbulence with supercomputers. *Sci. Am.* 276(1): 62-68.
4. Mullins, J. 1997. Secrets of a perfect skin. *New Sci.* 153(2065): 28-31.
5. Dadswell, M. J., and D. Weihs. 1990. Size-related hydrodynamic characteristics of the giant scallop *Placopecten magellanicus* (Bivalvia: Pectinidae). *Can. J. Zool.* 68: 778-785.
6. Cheng, J.-Y., and M. E. DeMont. 1996. Hydrodynamics of scallop locomotion: unsteady fluid forces on clapping shells. *J. Fluid Mech.* 317: 73-90.
7. Cheng, J.-Y., and M. E. DeMont. 1996. Jet-propelled swimming in scallops: swimming mechanics and ontogenic scaling. *Can. J. Zool.* 74: 1734-1748.
8. Cheng, J.-Y., I. G. Davison, and M. E. DeMont. 1996. Dynamics and energetics of scallop locomotion. *J. Exp. Biol.* 199: 1931-1946.
9. Vogel, S. 1997. Squirt smugly, scallop. *Nature* 385: 21-22.
10. Reif, W.-E. 1982. Morphology and hydrodynamic effects of the scales of fast swimming sharks. *Neues. Jahrb. Geol. Paleontol.* 164: 184-187.
11. Bechert, D. W., G. Hoppe, and W.-E. Reif. 1985. On the drag reduction of shark skin. *AIAA Paper* 85-0546.
12. Kline, S. J., W. C. Reynolds, F. A. Schraub, and P. W. Runstadler. 1967. The structure of turbulent boundary layers. *J. Fluid Mech.* 30: 741-773.
13. Djenidi, L., and R. A. Antonia. 1993. Riblet flow calculation with a low Reynolds number  $k-\epsilon$  model. *Appl. Sci. Res.* 50: 267-282.
14. Walsh, M. J. 1982. Turbulent boundary layer drag reduction using riblets. *AIAA Paper* 82-0169.



# BHL

## Biodiversity Heritage Library

Anderson, Erik J., MacGillivray, Patrick S., and Demont, M E. 1997. "Scallop Shells Exhibit Optimization of Riblet Dimensions for Drag Reduction." *The Biological bulletin* 192, 341–344. <https://doi.org/10.2307/1542744>.

**View This Item Online:** <https://www.biodiversitylibrary.org/item/17361>

**DOI:** <https://doi.org/10.2307/1542744>

**Permalink:** <https://www.biodiversitylibrary.org/partpdf/32092>

### **Holding Institution**

MBLWHOI Library

### **Sponsored by**

MBLWHOI Library

### **Copyright & Reuse**

Copyright Status: In copyright. Digitized with the permission of the rights holder.

Rights Holder: University of Chicago

License: <http://creativecommons.org/licenses/by-nc-sa/3.0/>

Rights: <https://biodiversitylibrary.org/permissions>

This document was created from content at the **Biodiversity Heritage Library**, the world's largest open access digital library for biodiversity literature and archives. Visit BHL at <https://www.biodiversitylibrary.org>.